Electronic Supplementary Information

Fine-tuning the type of equatorial donor atom in pentagonal bipyramidal Dy(III) complexes to enhance single-molecule magnet properties

Haipeng Wu,[‡] Min Li,[‡] Bing Yin,* Zhengqiang Xia,* Hongshan Ke, Qing Wei, Gang Xie, Sanping Chen* and Shengli Gao

[a] Key Laboratory of Synthetic and Natural Functional Molecule Chemistry of Ministry of Education, College of

Chemistry and Materials Science, Northwest University, Xi'an, 710127, China.

[‡] These authors contributed equally to this work.

*Corresponding authors

Prof. Bing Yin

E-mail: rayinyin@nwu.edu.cn

Dr. Zhengqiang Xia

E-mail: northwindy@126.com

Prof. Sanping Chen

E-mail: sanpingchen@126.com

1. Crystal Data and Structures

Table S1. Crystal data and structure refinement summary for complexes **1-3** and **1CH$_3$**.

	1	**2**	**3**	**1CH$_3$**
Empirical formula	C$_{14}$H$_{18}$Cl$_3$DyN$_4$	C$_{26}$H$_{22}$Br$_4$ClDyN$_6$O$_6$	C$_{96}$H$_{72}$Cl$_{18}$Dy$_3$N$_{21}$O$_{27}$	C$_{16}$H$_{22}$Cl$_3$DyN$_4$
Formula weight	511.17	1032.08	3077.34	539.22
Crystal system	Monoclinic	Triclinic	Monoclinic	Monoclinic
Temperature (K)	296.15 K	293 K	100 K	296.15 K
Space group	$P2_1$/c	$P\bar{1}$	$P2_1$/c	$P2_1$
a (Å)	11.8991(12)	8.2337(8)	23.3141(7)	8.5713(10)
b (Å)	9.1987(9)	11.3866(8)	18.7255(6)	14.3669(17)
c (Å)	16.9903(17)	18.9912(14)	26.6532(7)	8.9521(10)
α (º)	90	93.466(6)	90	90
β (º)	90.659(2)	95.632(7)	90.3870(10)	115.407(2)
γ(º)	90	110.499(9)	90	90
V (Å^3)	1859.6(3)	1651.1(3)	11635.7(6)	995.8(2)
Z	4	2	4	2
D_c (g m^{-3})	1.826	2.076	1.757	1.798
μ (mm^{-1})	4.449	18.939	2.401	4.16
F (000)	988	982	6060	526
Reflns	10044/3991	10925/5812	112854/23605	5335/3619
R_{int}	0.0260	0.0727	0.0559	0.0181
GOF on F^2	1.031	1.105	1.057	0.922
$R_1{}^a$ [$I > 2\sigma(I)$]	0.0254	0.0801	0.0744	0.0181
$wR_2{}^b$ (all data)	0.0560	0.1924	0.1879	0.0444
CCDC	1910325	1910326	1910327	1911489

$^aR_1 = \Sigma(|| F_o | -| F_c ||)/\Sigma| F_o |$. $^bwR_2 = [\Sigma w(F_o{}^2 - F_c{}^2)^2/\Sigma w(F_o{}^2)^2]^{1/2}$.

Table S2. Shape analysis for the metal centers of complexes **1-3** and **1CH$_3$**.

complex **1**	HP-7	HPY-7	PBPY-7	COC-7	CTPR-7	JPBPY-7	JETPY-7
Dy1	34.504	26.067	**0.828**	8.465	6.650	4.865	23.873

complex **2**	HP-7	HPY-7	PBPY-7	COC-7	CTPR-7	JPBPY-7	JETPY-7
Dy1	32.271	23.094	**2.086**	6.915	5.598	3.353	19.154

complex **3**	HP-7	HPY-7	PBPY-7	COC-7	CTPR-7	JPBPY-7	JETPY-7
Dy1	33.468	23.367	**1.114**	7.347	5.675	2.696	22.901
Dy2	32.750	23.469	**1.090**	6.685	4.879	2.896	21.517
Dy3	33.39	23.553	**0.808**	8.505	6.782	2.497	23.578

complex **1CH$_3$**	HP-7	HPY-7	PBPY-7	COC-7	CTPR-7	JPBPY-7	JETPY-7
Dy1	33.736	25.052	**0.795**	6.655	4.793	4.632	23.234

HP-7 (D_{7h}): Heptagon

HPY-7 (C_{6v}): Hexagonal pyramid

PBPY-7 (D_{5h}): Pentagonal bipyramid

COC-7 (C_{3v}): Capped octahedron

CTPR-7 (C_{2v}): Capped trigonal prism

JPBPY-7 (D_{5h}): Johnson pentagonal bipyramid J13

JETPY-7 (C_{3v}): Johnson elongated triangular pyramid J7

Table S3. Comparison of some crucial structural data for Schiff base complexes (**1'-3'**), reductive Schiff base complexes (**1-3**) and methylated complex (**1CH$_3$**).

Parameters	1'	1	1CH$_3$
Dy-N$_{imine}$/Dy-N$_{amine}$ (Å)	2.467(2)/2.481(2)	2.491(3)/2.510(3)	2.596(4)/2.579(4)
Dy-N$_{equatorial}$ (average) (Å)	2.5095	2.5325	2.572
Dy-O/Dy-Cl$_{equatorial}$ (Å)	2.6112(11)	2.6237(10)	2.6186(16)
Dy-O/Dy-Cl$_{axial}$ (Å)	2.5949(9)/2.6351(9)	2.5964(10)/2.6222(9)	2.6245(16)/2.5913(14)
∠O-Dy-O/Cl-Dy-Cl (°)	168.52(2)	170.40(3)	171.06(5)
r.m.s. deviation[a] of tetradentate coordination atoms	0.1342	0.0060	0.1059
r.m.s. deviation of pentagon coordination atoms	0.1875	0.0549	0.1387

Parameters	2'	2	3'	3
Dy-N$_{imine}$/Dy-N$_{amine}$ (Å)	2.490(8)	2.538(12)/2.517(10)	2.493(3)/2.494(3)	2.494
Dy-N$_{equatorial}$ (average) (Å)	2.523	2.5345	2.520	2.5166
Dy-O/Dy-Cl$_{equatorial}$ (Å)	2.616(3)	2.620(3)	2.203(2)	2.202
Dy-O/Dy-Cl$_{axial}$ (Å)	2.174(4)	2.175(7)/2.200(8)	2.187(2)/2.201(2)	2.187
∠O-Dy-O/Cl-Dy-Cl (°)	165.6(3)	173.4(3)	166.06(8)	167.87
r.m.s. deviation of tetradentate coordination atoms	0.2049	0.0054	0.2111	0.0956
r.m.s. deviation of pentagon coordination atoms	0.1833	0.2521	0.2235	0.0899

[a] Deviations from the Least-squares planes defined by tetradentate and pentagon coordination atoms.
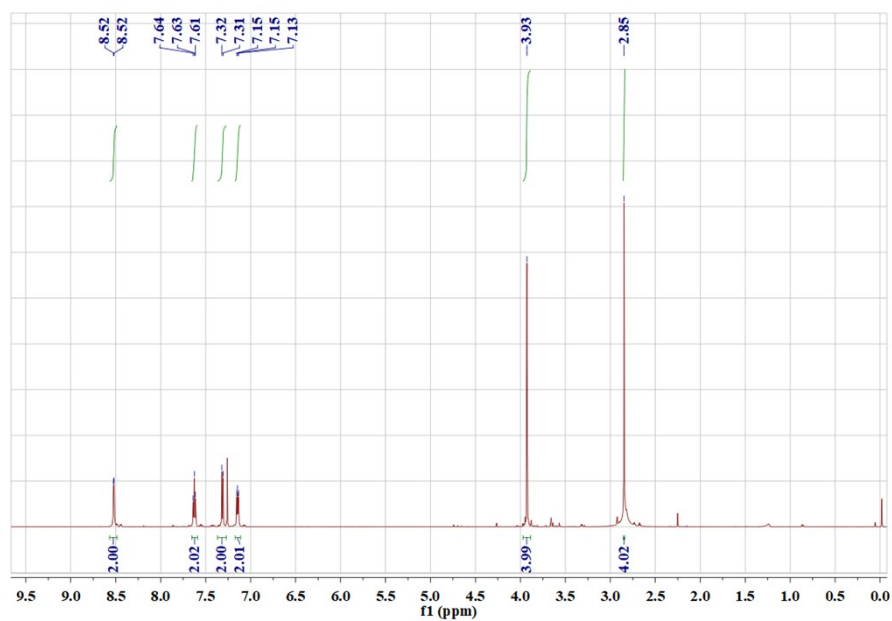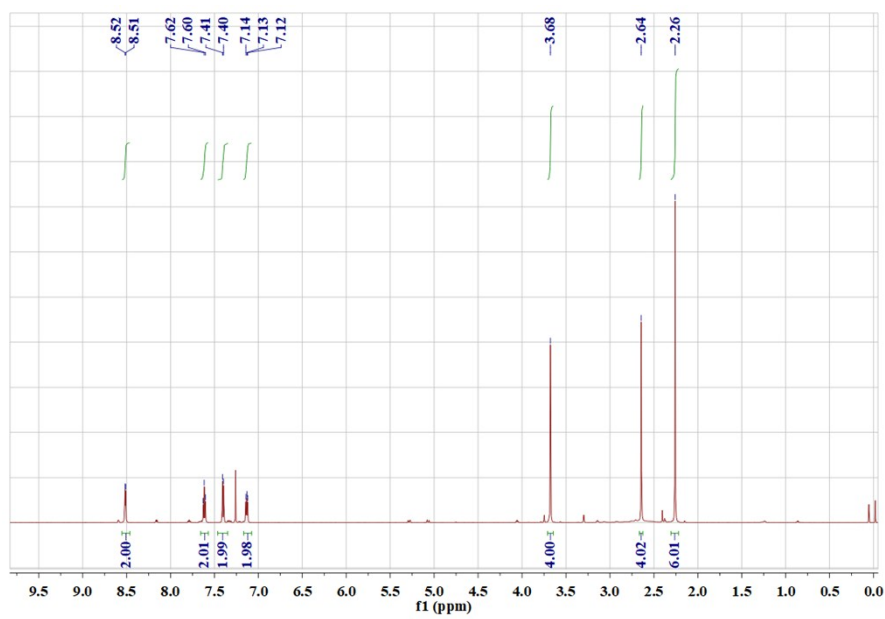
Fig. S1. ¹H NMR spectrum of Hbpen.

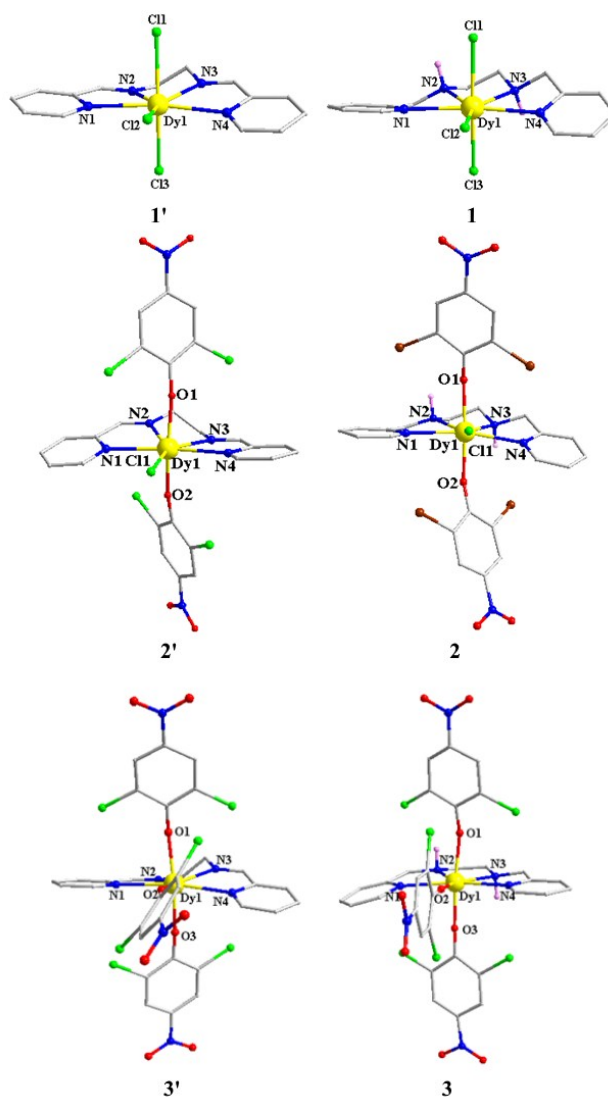**Fig. S2**. ¹H NMR spectrum of Mbpen.

Fig. S3. Coordination environment of the Dy^{III} center for Schiff base complexes **1'-3'** and reductive Schiff base complexes **1-3**. Yellow, blue, red, green, brown, light grey and light pink spheres represent Dy, N, O, Cl, C and H, respectively; non-amino hydrogen atoms and counter ions are removed for clarity.
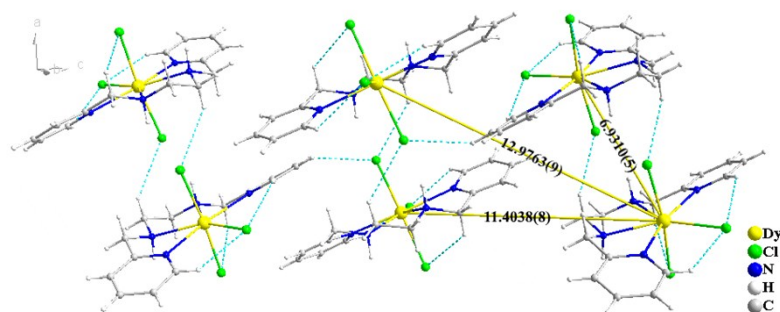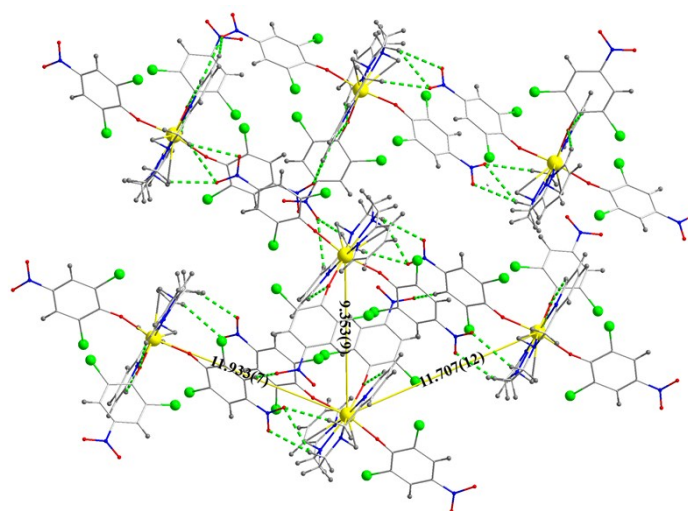

Fig. S4. The supramolecular network for **1**. The dash lines correspond intramolecular or intermolecular hydrogen bond (Cl···H-C). The yellow solid lines correspond the adjacent distances (Å) of Dy^{III} ions in **1**.
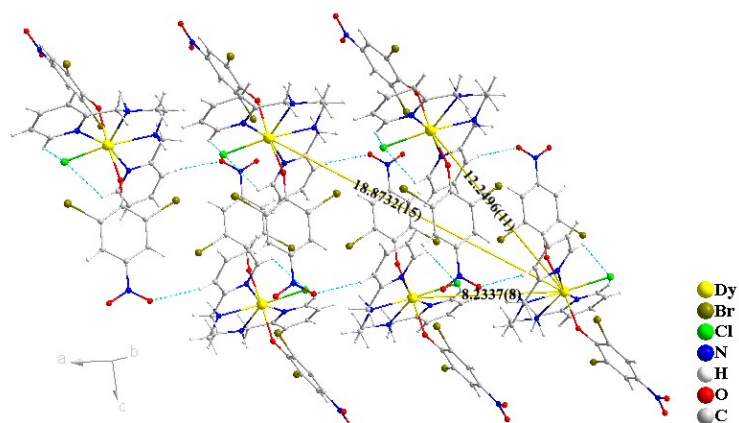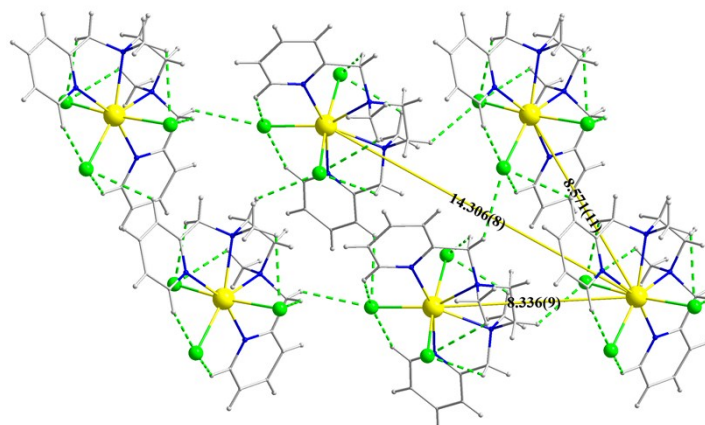
Fig. S5. The supramolecular network for **2**. The dash lines correspond intramolecular (Cl···H-C) and intermolecular hydrogen bond (O···H-C). The yellow solid lines correspond the adjacent distances (Å) of Dy^{III} ions in **2**.

Fig. S6. The supramolecular network for **3**. The dash lines correspond intramolecular or intermolecular hydrogen bond (O···H-C). The yellow solid lines correspond the adjacent distances (Å) of Dy^{III} ions in **3**.

Fig. S7. The supramolecular network for **1CH₃**. The dash lines correspond intramolecular or

intermolecular hydrogen bond (Cl···H-C). The yellow solid lines correspond the adjacent distances (Å) of Dy^{III} ions in **1CH$_3$**.
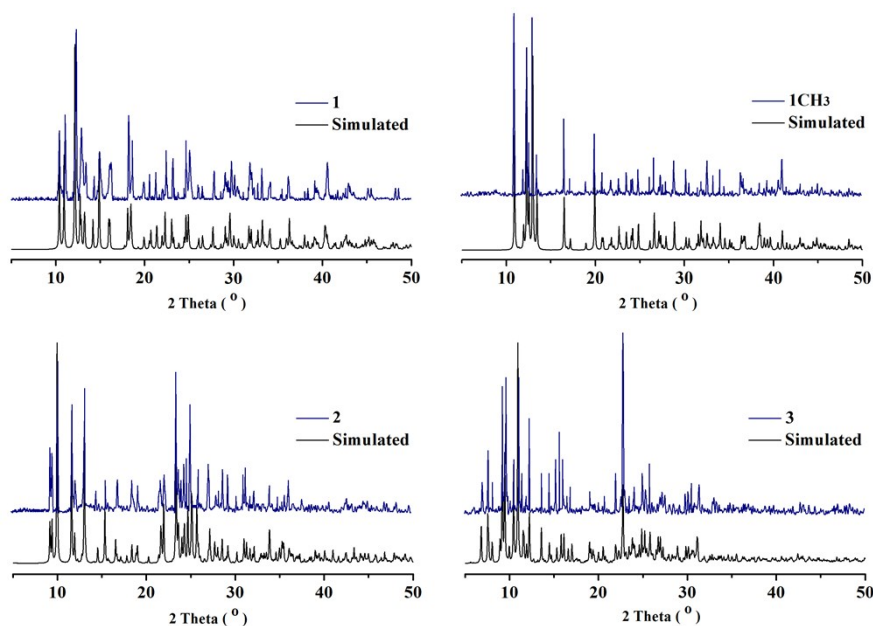

Fig. S8. Experimental X-ray powder diffraction patterns for **1-3** and **1CH$_3$** at room temperature.
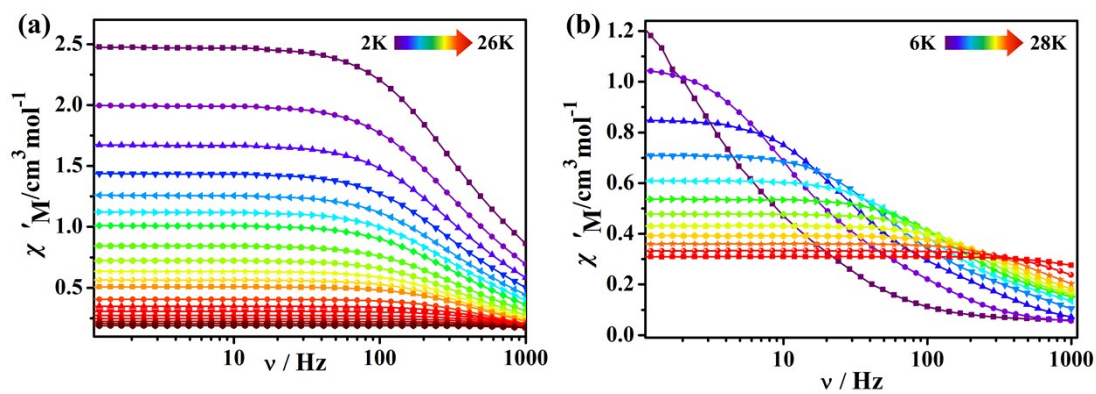
2. Magnetic measurements

Fig. S9. Frequency dependence of the in-phase χ' ac susceptibility signals for **2** under 0 Oe (a) and 1200 Oe (b) dc fields.
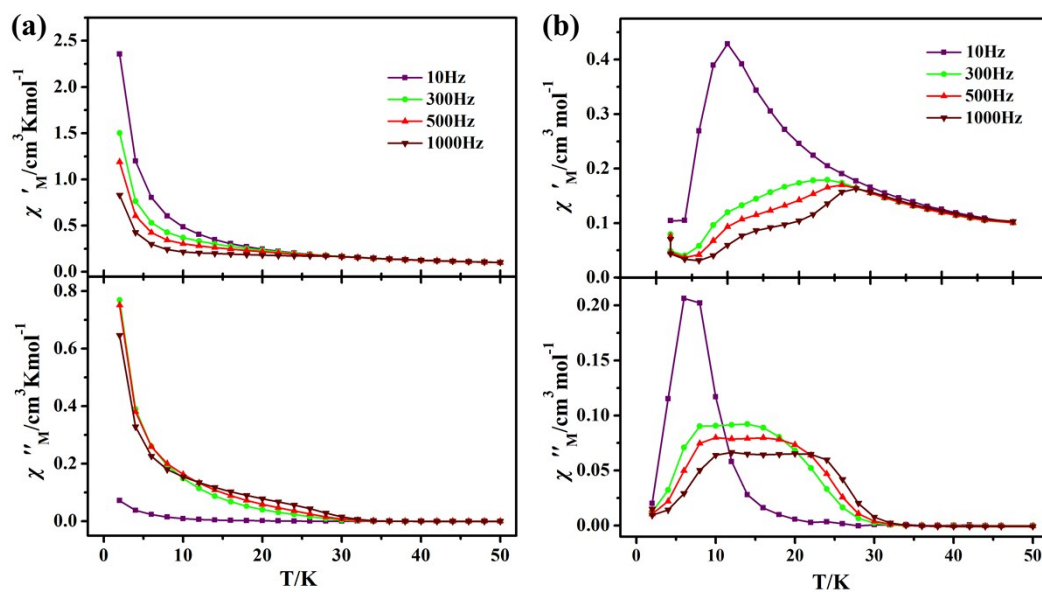
Fig. S10. Temperature-dependent in-phase χ′ (top) and out-of-phase χ″ (bottom) ac susceptibility signals for **2** under 0 Oe (a) and 1200 Oe (b) dc fields.
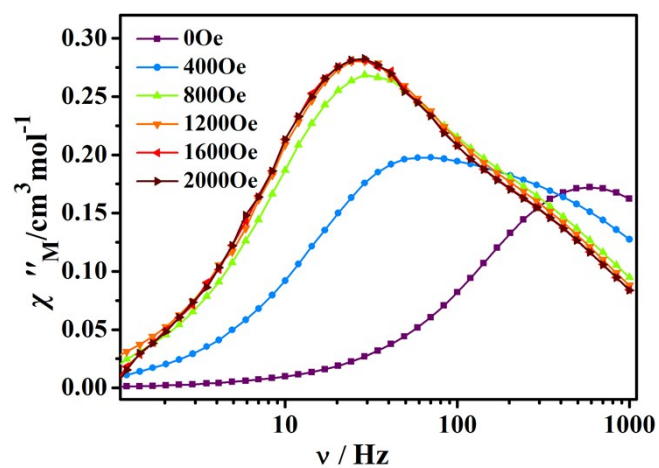

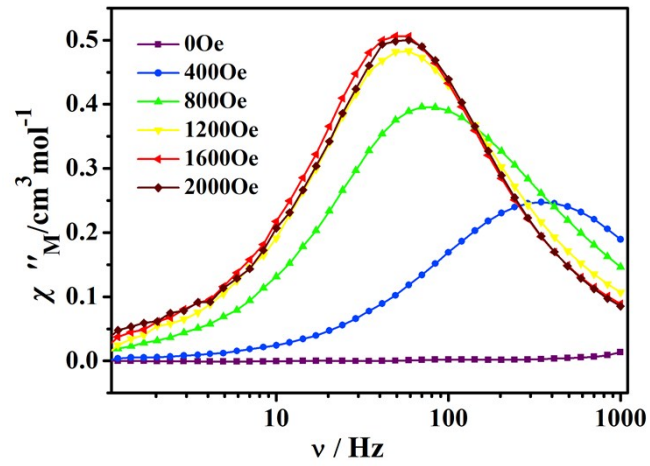**Fig. S11**. Field dependence of the out-of-phase signal vs frequency at 10 K for **2**.

Fig. S12. Field dependence of the out-of-phase signal vs frequency at 5 K for **1**.
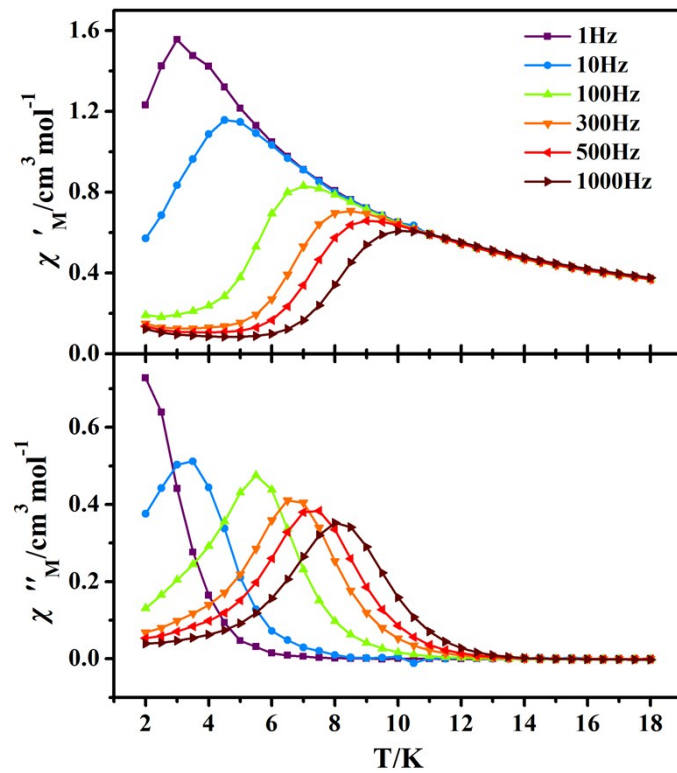

Fig. S13. Temperature-dependent in-phase χ′ (top) and out-of-phase χ″ (bottom) ac susceptibility signals under 1600 Oe dc field for **1**.
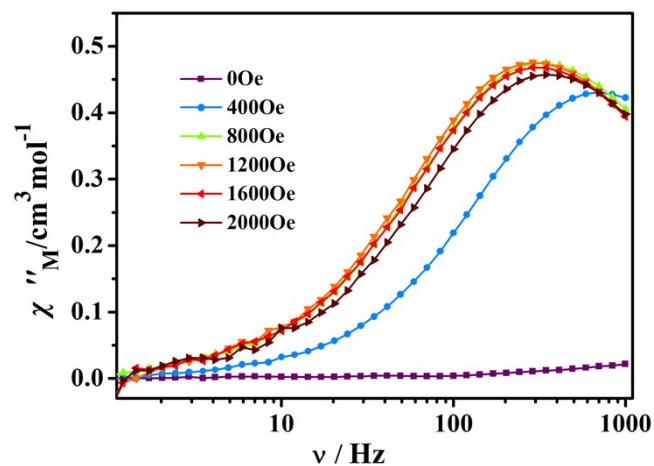
Fig. S14. Field dependence of the out-of-phase signal vs frequency at 5 K for **3**.

Fig. S15. Temperature-dependent in-phase χ' (top) and out-of-phase χ'' (bottom) ac susceptibility signals under 1200 Oe dc field for **3**.

Fig. S16. Field dependence of the out-of-phase signal vs frequency at 3.5 K for **1CH₃**.
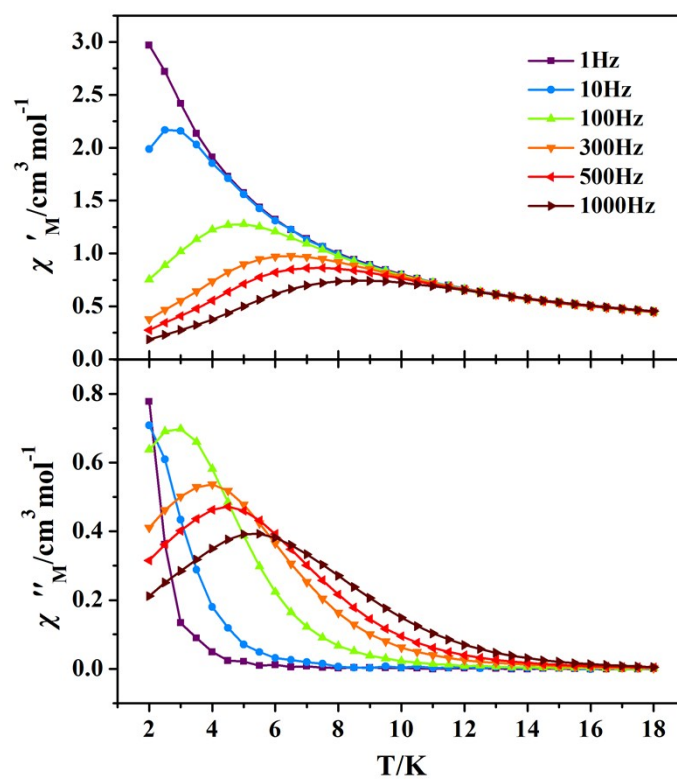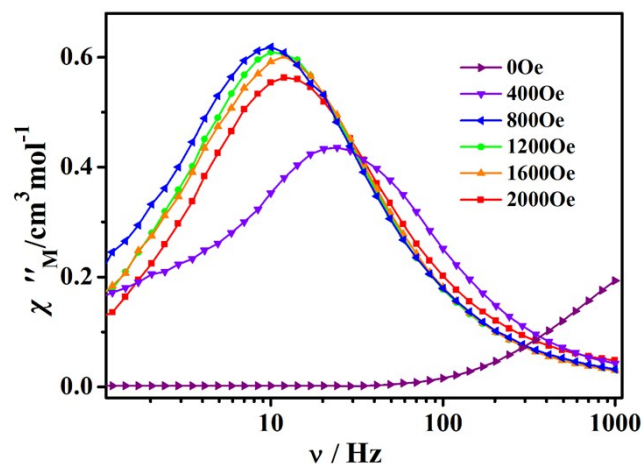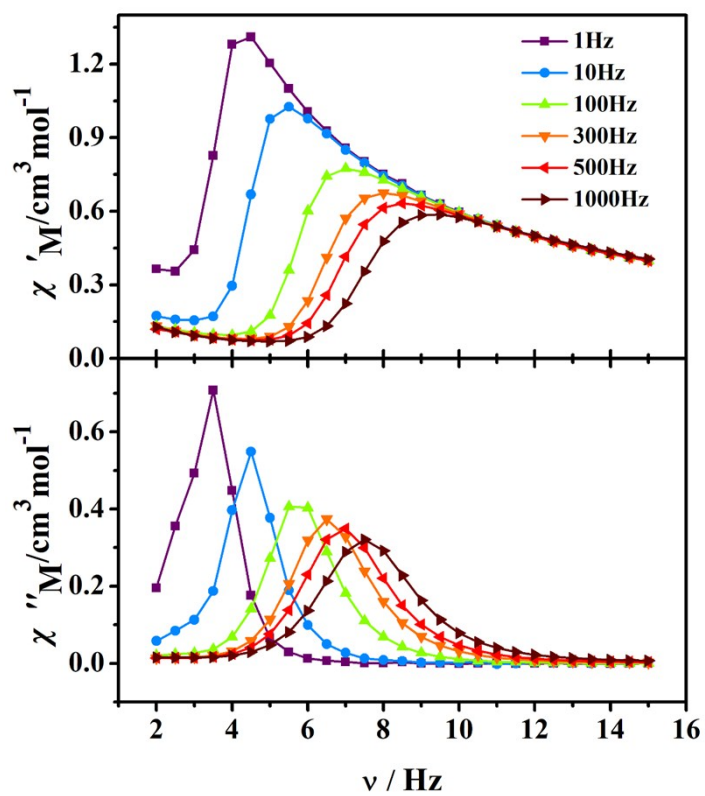

Fig. S17. Temperature-dependent in-phase χ' (top) and out-of-phase χ'' (bottom) ac susceptibility signals under 800 Oe dc field for **1CH₃**.
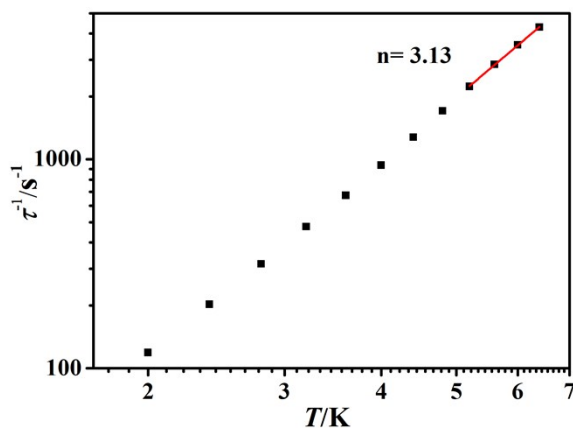
Fig. S18. The plots of τ^{-1} *vs.* T in a log-log scale for **3** under 1200 Oe dc field. The solid lines are fitness by a power law with parameters n = 3.13 above 5.2 K.
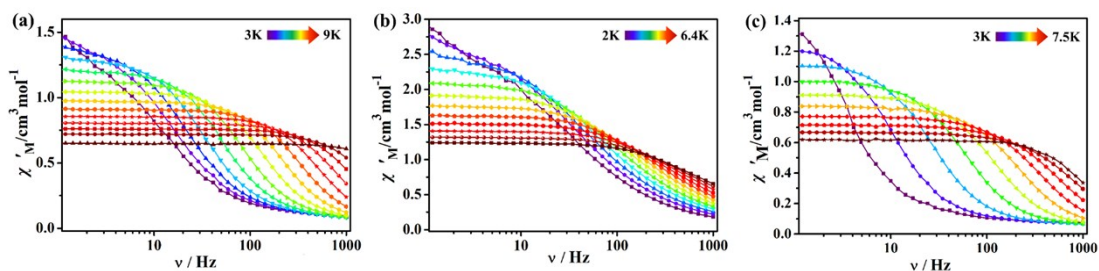
Fig. S19. Frequency dependence of the in-phase χ' ac susceptibility signals for **1** under 1600 Oe dc field (a), for **3** under 1200 Oe dc field (b) and for **1CH$_3$** under 800 Oe dc field (c).
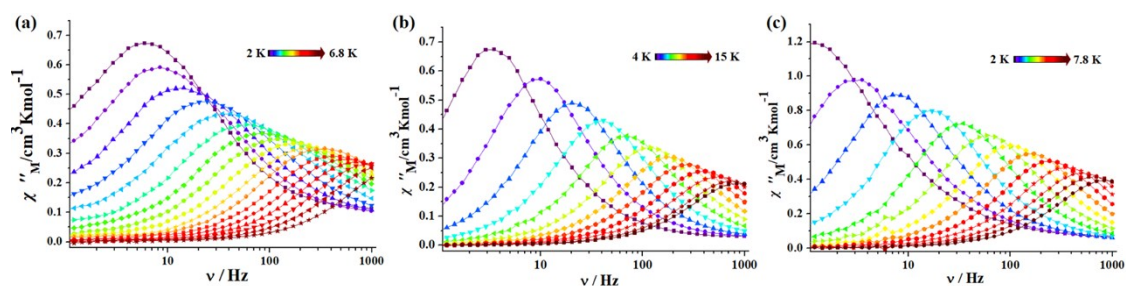
Fig. S20. Frequency-dependent out-of phase χ'' ac susceptibility signals for reported complexes **1'** (a)**, 2'** (b) and **3'** (c).

Table S4. Comparison of magnetic properties for Schiff base complexes (**1'-3'**), reductive Schiff base complexes (**1-3**) and methylated complex (**1CH$_3$**).

Complex	U_{eff}(K)	H_{dc}/Oe	Hysteresis (K)
1'	22.4	800	-

11

1	63.4	1600	-
1CH$_3$	37.1	800	-
2'	85.8	1000	-
2	181.7	0	3
	254.2	1200	
3'	34.2	800	-
3	[a]21.3	1200	-

[a] The experimentally determined apparent energy barrier value.

3. *Ab initio* calculations

Multiconfigurational ab initio calculations, including spin-orbit coupling (SOC), were performed on the experimental structures of **1-3** and **1CH$_3$** to explore their magnetic anisotropy. This type of calculation consists of two steps [1]: 1) a set of SOC-free states, that is, spin eigenstates, are obtained by the CASSCF method; 2) the lowlying SOC states, that is, Kramers doublets (KD) herein, are obtained by state interaction, i.e., diagonalizing the SOC matrix in the space spanned by the spin eigenstates from the first step. All calculations were carried out with the MOLCAS@UU, a freely distributed version of MOLCAS 8.0 program.[2,3] In the CASSCF step, the active space consisted of 9 electrons in 7 orbitals and all the spin eigenstates of 21 sextets were included. Due to the limitation in the aspect of hardware, other highly excited quartets and doublets were not considered. The subsequent step of state interaction was performed by the RASSI-SO module. The ANO-RCC basis sets, including VTZP for Dy, VDZ for C and H as well as VDZP for other atoms, were used. The extraction procedure according to Chibotaru *et. al.* was performed to obtain the g-tensors and transition magnetic moments of low-lying KDs with the SINGLE ANISO module.[4,5]
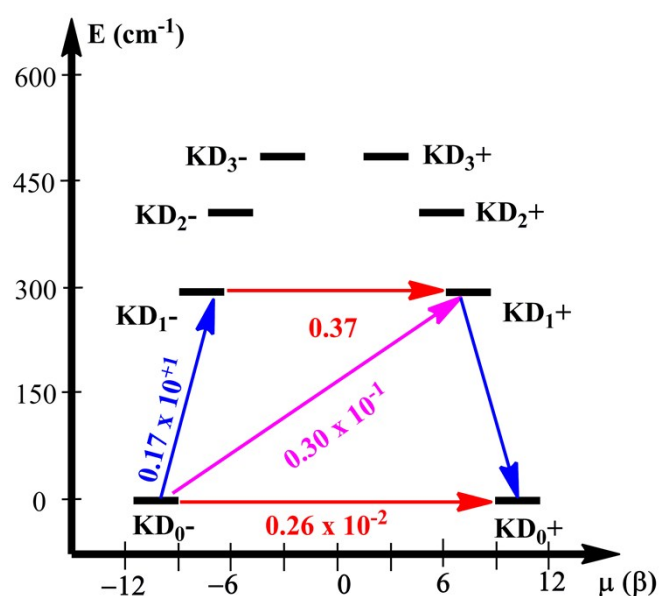

Fig. S21 *Ab initio* predicted effective energy barriers for complex **2** with the red arrows indicating the possibility of QTM and the blue and pink arrows indicating the possibilities of other processes of spin–phonon relaxation.

Table S5. Natural Population Analysis (NPA) charge from the LoProp module of MOLCAS code of selected atoms for complexes **1'-3'**, **1-3** and **1CH₃**.

coordination atoms	charge(a.u.) 1'	1	1CH₃	coordination atoms	charge(a.u.) 2'	2	coordination atoms	charge(a.u.) 3'	3
Cl1	-0.862	-0.862	-0.8614	O1	-0.855	-0.845	O1	-0.852	-0.887
Cl3	-0.867	-0.866	-0.8617	O2	-0.855	-0.875	O2	-0.850	-0.833
Cl2	-0.863	-0.860	-0.8574	Cl1	-0.862	-0.859	O3	-0.859	-0.880
N1	-0.321	-0.348	-0.3474	N1	-0.315	-0.346	N1	-0.324	-0.337
N4	-0.322	-0.346	-0.3483	N4	-0.315	-0.351	N4	-0.323	-0.348
N2	**-0.322**	**-0.418**	**-0.2978**	**N2**	**-0.325**	**-0.413**	**N2**	**-0.320**	**-0.410**
N3	**-0.318**	**-0.415**	**-0.3005**	**N3**	**-0.325**	**-0.418**	**N3**	**-0.314**	**-0.422**

Table S6. The nearest-neighbour distances r_{nn} and use the value R, which is the sum of all the nearest-neighbour r_{nn}^{-3}, as a semi-quantitative parameter describing the internal dipolar field.

3'		3	
$r_{nn\,(in\,Å)}$	r_{nn}^{-3}	$r_{nn\,(in\,Å)}$	r_{nn}^{-3}
9.961	0.001011792	9.353	0.001222214
10.323	0.000909038	9.804	0.001061183
10.5	0.000863838	10.859	0.000780963
10.586	0.000842955	10.918	0.000768371
11.377	0.000679073	11.141	0.000723148
11.599	0.000640823	11.212	0.000709497
12.247	0.000544391	11.752	0.000616119
12.281	0.000539882	11.878	0.000596719
13.370	0.000418414	12.877	0.000468334
14.388	0.000335737	14.868	0.000304258
16.433	0.000225346	18.483	0.000158374
17.990	0.000171754	18.552	0.000156613
19.385	0.000137279	20.626	0.000113961
	$R = 0.007320321$		$R = 0.007679754$

4. References

1. J. Luzon and R. Sessoli, *Dalton trans.*, **2012**, *41*, 13556-13567.
2. F. Aquilante, L. De Vico, N. Ferré, G. Ghigo, P.-å. Malmqvist, P. Neogrády, T. B. Pedersen, M. Pitoňák, M. Reiher, B. O. Roos, L. Serrano-Andrés, M. Urban, V. Veryazov and R. Lindh, *J. Comput. Chem.*, **2010**, *31*, 224-247.
3. F. Aquilante, J. Autschbach, R. K. Carlson, L. F. Chibotaru, M. G. Delcey, L. De Vico, I. Fdez. Galván, N. Ferré, L. M. Frutos, L. Gagliardi, M. Garavelli, A. Giussani, C. E. Hoyer, G. Li Manni, H. Lischka, D. Ma, P. Å. Malmqvist, T. Müller, A. Nenov, M. Olivucci, T. B. Pedersen, D. Peng, F. Plasser, B. Pritchard, M. Reiher, I. Rivalta, I. Schapiro, J. Segarra-Martí, M. Stenrup, D. G. Truhlar, L. Ungur, A. Valentini, S. Vancoillie, V. Veryazov, V. P. Vysotskiy, O. Weingart, F. Zapata and R. Lindh, *J. Comput. Chem.*, **2016**, *37*, 506-541.
4. L. F. Chibotaru, *Adv. Chem. Phys.*, **2013**, *153*, 397-519.
5. L. F. Chibotaru and L. Ungur, *J. Chem. Phys.*, **2012**, *137*, 064112.